Organic & Biomolecular Chemistry

ROYAL SOCIETY OF CHEMISTRY

PAPER

View Article Online
View Journal | View Issue

Cite this: *Org. Biomol. Chem.*, 2020, **18**, 4773

Enhanced ion binding by the benzocrown receptor and a carbonyl of the aminonaphthalimide fluorophore in water-soluble logic gates†‡

Andreas Diacono, Marie Claire Aquilina, Andrej Calleja, Godfrey Agius, Gabriel Gauci, Konrad Szaciłowski and David C. Magri *

Received 10th January 2020,
Accepted 24th March 2020

DOI: 10.1039/d0ob00059k

rsc.li/obc

Two fluorescent logic gates **1** and **2** were designed and synthesised with a '*receptor*$_1$-*spacer*$_1$-*fluorophore*-*spacer*$_2$-*receptor*$_2$' format. The molecules comprise of an aminonaphthalimide fluorophore, methylpiperazine and either benzo-15-crown-5 or benzo-18-crown-6. Model **3**, with a weakly binding 3,4-dimethoxyphenyl moiety, was also synthesised. The compounds were studied both in 1 : 1 (v/v) methanol/water and water by UV-visible absorption and steady-state fluorescence spectroscopy. The green fluorescence of **1–3** is modulated by photoinduced electron transfer (PET) and internal charge transfer (ICT) mechanisms, and by solvent polarity. In 1 : 1 (v/v) methanol/water, logic gates **1** and **2** emit with Φ_f = 0.21 and 0.28, and bind with pβ_{Na^+} = 1.6 and pβ_{K^+} = 2.6, respectively, and pβ_{H^+} = 7.4 ± 0.1. In water, logic gates **1** and **2** emit with Φ_f = 0.14 and 0.26, and bind with pβ_{Na^+} = 0.86 and pβ_{K^+} = 1.6, respectively, and pβ_{H^+} = 8.1 ± 0.1. The measured pβ_{Na^+} are significantly lower than reported for analogous classic anthracene-based Na^+, H^+-driven AND logic gates indicating a stronger Na^+ binding interaction, which is attributed to direct interaction with one carbonyl moiety within the aminonaphthalimide. Supporting evidence is provided by DFT calculations. Furthermore, we illustrate an example of logic function modulation by a change in solvent polarity. In 1 : 1 (v/v) methanol/water, molecules **1** and **2** function as Na^+, H^+ and K^+, H^+-driven AND logic gates. In water, the molecules function as single input H^+-driven YES logic gates, while consideration as two-input devices, **1** and **2** function as AND-INH-OR logic arrays.

Introduction

Molecular logic-based computation[1] emerged in 1993 with the first molecular AND logic gate by de Silva.[2] Purposely designed according to a '*fluorophore-spacer*$_1$-*receptor*$_1$-*spacer*$_2$-*receptor*$_2$' format, an anthracene fluorophore was linked by methylene spacers to a proton-accepting aliphatic amine (*receptor*$_1$) and a benzo-15-crown-5 (*receptor*$_2$) for binding H^+ and Na^+, respectively. Four years later, an improved prototype embodying the same modular units, but arranged in a '*receptor*$_1$-*spacer*$_1$-*fluorophore*-*spacer*$_2$-*receptor*$_2$' format (Fig. 1) gave a much brighter turn-on fluorescence.[3] The breakthrough resulted from shortening the distance for photoinduced electron transfer (PET) between the fluorophore and the two receptors.[4] The hydro-

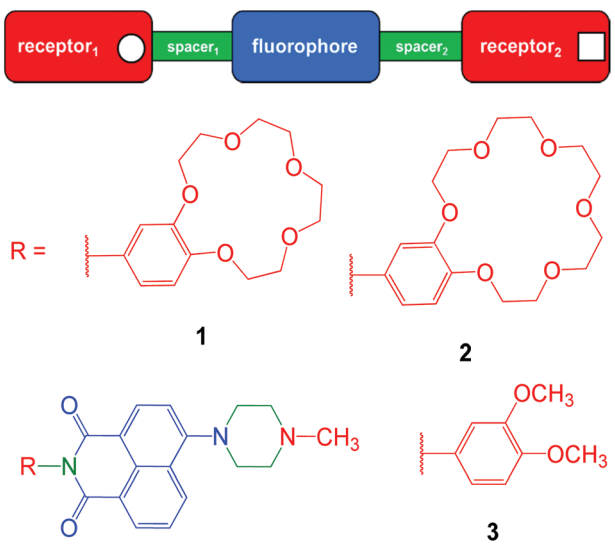

Fig. 1 The colour-coded design concept[4] (top) and molecular structures (bottom) of the logic gates **1–3**. The inputs are Na^+ or K^+ (receptor$_1$) and H^+ (receptor$_2$). Spacer$_1$ is a virtual C_0-type spacer, while spacer$_2$ is a diethylene (C_2) spacer.

Department of Chemistry, Faculty of Science, University of Malta, Msida, MSD 2080, Malta. E-mail: david.magri@um.edu.mt; https://www.um.edu.mt/profile/davidmagri

†This paper is a contribution on The Mechanics of Supramolecular Chemistry to commemorate the 60th birthday of Eric Anslyn.

‡Electronic supplementary information (ESI) available: Synthetic and experimental details, UV-visible absorption, fluorescence, ^{1}H & ^{13}C NMR, IR, mass spectra and truth Table S1. See DOI: 10.1039/d0ob00059k

phobic nature of anthracene, though, restrained these first demonstrations of molecular logic to alcoholic solutions.

Now over a quarter of a century later, the field of molecular logic-based computation is focusing on two significant challenges. The first challenge is the development of tools for pragmatic uses.[5] For example, crown-ether containing molecules,[6] including M^+/H^+ logic gates, are applicable as smart fluorescent probes for investigating biological membrane interfaces, M^+/H^+ antiporters,[7] protein interactions[8] and theranostics.[9] The second challenge is the development of molecular tools that function in water.[5] Overcoming these issues requires the application of physical organic chemistry principles.[10] For instance; the mechanism of fluorescence enhancement in boronic acid saccharide sensors has been a topic of debate.[11] The original paradigm postulated for *ortho*-aminomethylphenylboronic acid chemosensors was a PET mechanism and a B–N bonding interaction upon sugar binding.[12] The latest evidence with anthracene and 4-aminonaphthalimide models points to a solvent-induced effect *via* a vibrational-coupled excited-state relaxation mechanism.[11a]

While anthracene is an example of a fluorophore with a pure π–π* excited state, aminonaphthalimide is an example with an π–π* internal charge transfer (ICT) and a photoelectric field effect in the excited state.[12] *N*-Aryl-aminonaphthalimides are also intriguing, because of the virtual C_0-type spacer as a result of a frontier orbital node at the imide nitrogen atom.[14] Typically PET systems (*i.e.* de Silva's first AND logic gates)[2,4] are designed with methylene (C_1) spacers, which allows for some degree of conformational mobility. However, the π molecular orbitals of the aminonaphthalimide fluorophore, and those of the *N*-aryl receptor, preferentially adopt an orthogonal geometry to prevent steric clash. Such systems are often described as possessing a non-emissive twisted internal charge transfer (TICT) excited state.[15]

Most naphthalimide-based chemosensors with crown ethers have been studied in organic solvents.[16] Fedorova and co-workers have reported many examples of benzo-15-crown-5 and aza-crowns in acetonitrile.[17] Studies in aqueous methanol or water, however, are limited to an azadithiacrown (for Hg^{2+}),[18] and *N*-phenylaza-dithia-15-crown-5 (for Ag^+),[19] an aza-15-crown-5 (for Hg^{2+})[20] and benzo-15-crown-5 and benzo-18-crown-6 (for Na^+ and K^+).[21]

Our curiosity was stimulated by the Heagy study.[21] Benzo-15-crown-5 and benzo-18-crown-6 were attached at the *N*-imide position of a 1,8-naphthalic anhydride while a sulfonate moiety was attached at the 4-position. Apparent binding constants of 1.12 mM ($p\beta_{Na^+} = 2.95$) and 0.4 mM ($p\beta_{K^+} = 3.40$) were measured in buffered water with the benzo-15-crown-5 and benzo-18-crown-6 chemosensors, respectively. The selectivity for the Na^+ probe is admirable better than the *N*-(2-methoxyphenyl)aza-15-crown-5 receptor with its pendant methoxy moiety,[22] which is used to monitor Na^+ blood serum levels.[23] We hypothesised that the enhanced selectivity and sensitivity for Na^+ binding by the benzo-15-crown-5, as reported by Heagy,[21] is due to Na^+ coordinating with at least one naphthalimide carbonyl moiety.

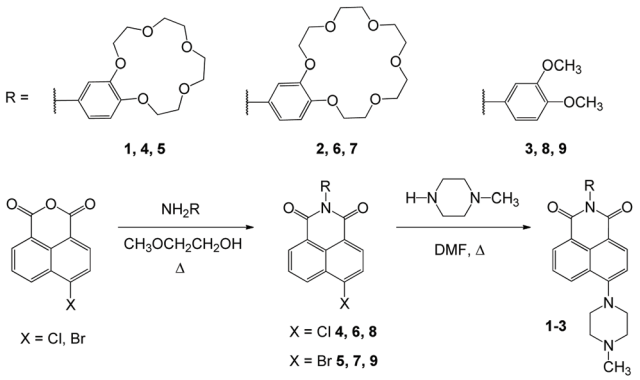

Scheme 1 Synthetic protocols for the naphthalimide-based molecular logic gates **1–3**.

Hence, we set out to develop molecular AND logic gates for biologically relevant analytes in water to exploit the concept of fluorophore-assisted binding. Herein we report the synthesis and photophysics of novel compounds **1–3** that function as Na^+, H^+ and K^+, H^+ logic gates in aqueous methanol and water (Fig. 1). Molecules **1** and **2** are designed with a *receptor*$_1$-*spacer*$_1$-*fluorophore-spacer*$_2$-*receptor*$_2$ format with an aminonaphthalimide fluorophore; a methylpiperazine H^+ receptor; and either a benzo-15-crown-5 or benzo-18-crown-6 receptor, principally for binding Na^+ and K^+, respectively (Scheme 1). Compound **3**, containing a 3,4-dimethoxyphenyl moiety, is included for comparison.

Results and discussion

The syntheses of **1–3** are shown in Scheme 1. 4-Bromo-1,8-naphthalic anhydride or 4-chloro-1,8-naphthalic anhydride were reacted with 4′-aminobenzo-15-crown-5, 4′-aminobenzo-18-crown-6 or 3,4-dimethoxyaniline in 2-methoxyethanol (or acetic acid) at 110 °C resulting in *N*-(benzo-15-crown-5)-4-bromo-1,8-naphthalimide **5**, *N*-(benzo-18-crown-6)-4-bromo-1,8-naphthalimide 7, and *N*-(3,4-dimethoxyphenyl)-4-bromo-1,8-naphthalimide **9** in 73%, 57% and 72% yields. The chloro-substituted analogues **4**, **6** and **8** were synthesised in 62%, 61% and 85%. The intermediates **4–9** were subsequently reacted with methylpiperazine in hot DMF to obtain the target compounds **1–3**. Products **1–3** were purified by column chromatography with dichloromethane/methanol and isolated as yellow, orange and yellow powders in 65%, 49% and 70% yield. Analytical spectroscopic data is provided in the Experimental section and the corresponding spectra are provided in the ESI (Fig. S1–S36‡).

Prior to performing the spectroscopic studies, we assessed the partition coefficients and PET thermodynamics of **1–3**. The octanol-water partition coefficients ($\log P$) of the logic gates were determined by the shake flask method.[24] Sample UV-visible absorption spectra from the extraction are provided in the ESI (Fig. S37 and S38‡). The experimental $\log P$ values of **1–3** are 0.097, −0.216 and 0.273, which are in good agreement

with the log *P* values of 0.15, 0.060 and 0.97 predicted for protonated **1–3** by ChemDraw Pro (version 12.19). The partition coefficients of the ionized species at pH 4.0 (log *D*) were calculated using eqn (1) based on a pK_a of 8.1. The log *D* values of **1–3** are indeed substantially more negative at −4.00, −4.32 and −3.83. Hence to our satisfaction, **1–3** were predicted to be fully soluble in water under acidic conditions. Our experimental results confirmed that **1–3** are indeed hydrophilic and readily dissolve in water in contrast to our prior study of an aza-crown anthracene-based logic gate.[25] We welcomed these findings as they provided quantitative evidence for shifting from 1 : 1 (v/v) aqueous methanol to water.

$$\log D = \log P + \log[1/(1 + 10^{(pK_a - pH)})] \quad (1)$$

The thermodynamics for the PET driving forces were calculated using the Weller equation, eqn (2), based on electrochemical and photophysical data.[4,26] The driving forces for PET from the tertiary amine and the 3,4-dimethoxyphenyl to the aminonaphthalimide fluorophore are 0.07 eV and 0.37 eV (6.7 and 35 kJ mol^{-1}), respectively, in acetonitrile (electrochemical data in methanol or water are not readily available). These values are mildly endothermic and susceptible to the influence of solvent polarity, which is accounted for in the Coulombic term $e^2/\varepsilon r$, where ε is the solvent dielectric constant. The ion-paring term $e^2/\varepsilon r$ was taken as 0.10 eV (10 kJ mol^{-1}) in acetonitrile.[27] The stabilization offered by the solvent to the radical ion pair after a PET process to a neutral molecule generally increases with solvent polarity.[27] Therefore, a change in solvent polarity, in this study from 1 : 1 MeOH/H_2O to water, could significantly alter the ΔG_{PET} such that PET from both receptors becomes less endothermic (more exothermic), and consequently, the fluorescence quantum yield decreases. The situation with 4-aminonaphthalimides, however, is not so clear-cut as the ICT pathway near the piperazyl is assisted by a photoexcited electric field effect,[28] while at the *N*-imide end, PET from the 3,4-dimethoxyphenyl to the excited fluorophore is hindered by a negative node at the imide nitrogen atom.

$$\Delta G_{PET} = E_{ox} - E_{red} - E_s - e^2/\varepsilon r \quad (2)$$

The UV-visible absorption spectra of **1–3** were first studied in both 1 : 1 (v/v) MeOH/H_2O and water as a function of pH with various cations including Na^+ and K^+ (Fig S39‡). Unprotonated **1–3** in water in the presence of 10^{-11} M H^+ has a λ_{max} at 400 nm ($\log \varepsilon$ = 3.91), which is not significantly affected in the presence of 200 mM Na^+. Upon addition of 10^{-4} M H^+, protonation of the piperazinyl nitrogen atom results in a hypsochromic (blue) and hyperchromic (increase) shift to a λ_{max} of 391 nm ($\log \varepsilon$ = 3.96). Titrations with acid between 10^{-11} M and 10^{-2} M H^+ reveals an isosbestic point at 412 nm (Fig. S40‡). The spectral shift is consistent with an excited state ICT due to charge repulsion between the protonated methylpiperazine and the positively charged pole at the 4-position. A summary of photophysical data is given in Table 1.

Table 1 Various parameters for **1–3** in 1 : 1 (v/v) methanol/water and water determined by UV-visible absorption and fluorescence spectroscopy[a,b]

Parameter	**1** MeOH/H_2O	**1** H_2O	**2** MeOH/H_2O	**2** H_2O	**3** MeOH/H_2O	**3** H_2O
$\lambda_{Abs\ pH\ 9}$/nm[c]	408	400	400	398	413	403
$\log \varepsilon_{pH\ 9}$[d]	3.99	3.70	3.99	3.91	4.00	3.94
$\lambda_{Abs\ pH\ 4}$/nm[c]	391	391	388	390	390	392
$\log \varepsilon_{pH\ 4}$[d]	4.09	4.07	4.09	3.96	4.12	3.92
λ_{isos}/nm	400	412	395	408	401	413
$\lambda_{flu\ pH\ 4}$/nm[c]	533	540	532	540	536	541
Φ_f[e]	0.21	0.14	0.28	0.26	0.05	0.08
FE[f]	26	4	11	6	3	4
$p\beta_{H^+}$[g]	7.5	8.2	7.4	8.0	7.4	7.2
$p\beta_{Na^+}$[g]	1.6	0.86	4.4[h]	1.8	0.88	0.18
$p\beta_{K^+}$[g]	1.3	0.76	2.6	1.6	—	—

[a] 10^{-5} μM **1** excited at λ_{isos}. [b] High H^+ level 10^{-4} M . Low H^+ level 10^{-9} M by addition of 0.10 M HCl or 0.10 M Bu_4NOH solution (25% wt in H_2O). [c] High Na^+ or K^+ 200 mM NaCl or KCl. Low Na^+ or K^+ level with no salt added. [d] Molar absorptivity ε in L mol^{-1} cm^{-1}. [e] Quantum yields measured with reference to quinine sulfate in 0.1 M H_2SO_4 water. [f] H^+-induced fluorescence enhancement (FE) $I_{F_{pH\ 4}}/I_{F_{pH\ 9}}$. [g] Determined by $\log[(I_{max} - I)/(I - I_{min})] = -\log[M^+] + \log \beta_{H^+}$ from emission spectra. [h] Value for 18-crown-6 in methanol. Ref. 6.

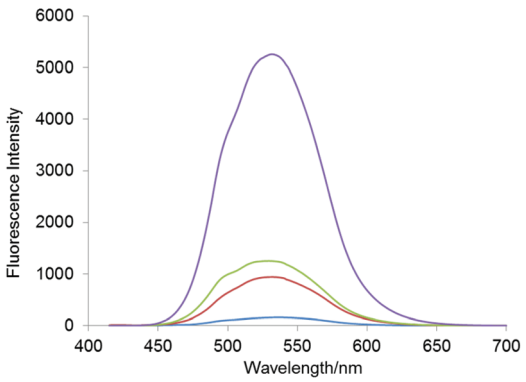

Fig. 2 Fluorescence spectra of 7 μM **1** in 1 : 1 (v/v) MeOH/H_2O at 10^{-9} M H^+ or 10^{-4} M H^+ and 200 mM M Na^+. See Table 2 for specific details.

The fluorescence spectra of **1** in 1 : 1 (v/v) MeOH/H_2O as a function of H^+ and/or Na^+ inputs are shown in Fig. 2. The peak maxima are observed at 525 nm, which is characteristic of a green coloured emission at high H^+ and Na^+ levels. Low threshold concentrations of H^+ or Na^+, or the absence of both H^+ and Na^+, results in little fluorescence at 10^{-9} M H^+. At a lower proton concentration of 10^{-11} M H^+, adjusted with 0.10 M Bu_4NOH solution, no emission is observed. In contrast, in the presence of excess threshold levels of H^+ and Na^+, the fluorescence is substantially high as shown for **1** in Fig. 2. A similar outcome was observed for **2** at high H^+ and K^+ levels. This pattern of three low and one high emission states exemplifies AND logic. Truth tables for **1** and **2**, including the quantum yields of fluorescence (Φ_f), are given in Table 2 and Table S1,‡ respectively.

Spectrofluorimetric pH titrations were performed for **1–3** at a constant ionic strength of 0.20 M salt in 1 : 1 (v/v) MeOH/

Table 2 Truth tables for logic gate **1** in 1 : 1 (v/v) methanol/water and water[a]

Input$_1$ (H^+)[b]	Input$_2$ (Na^+)[c]	Output Φ_F[d] MeOH/H_2O	Output Φ_F[d] H_2O
0 (low)	0 (low)	0 (low, 0.007)	0 (low, 0.020)
0 (low)	1 (high)	0 (low, 0.038)	0 (low, 0.066)
1 (high)	0 (low)	0 (low, 0.052)	1 (high, 0.11)
1 (high)	1 (high)	1 (high, 0.21)	1 (high, 0.14)

[a] 7 μM **1** excited at 405 nm. [b] High H^+ level 10^{-4} M. Low H^+ level 10^{-9} M by addition of 0.10 M HCl or 0.10 M Bu_4NOH solution (25% wt in H_2O). [c] High Na^+ level 200 mM NaCl. Low Na^+ level no NaCl added. [d] Quantum yields measured with reference to quinine sulfate in 0.1 M H_2SO_4 water.

H_2O and water. The binding constants were evaluated in the presence of excess amount of the other input (either 10^{-4} M H^+ or 0.20 M salt) such that the crown ether receptor would be saturated or the methylpiperazine fully protonated. The ion binding constants were determined from I_F-pM profiles[13] according to eqn (3)

$$\log[(I_{F_{max}}-I_F)/(I_F-I_{F_{min}})] = -\log[M^+]-\log \beta_{M^+} \quad (3)$$

where pM = $-\log[M^+]$ and M^+ is either H^+, Na^+ or K^+. From the I_F-pM titrations, the binding constants (pβ_{M^+}) were determined as the concentration at which half the receptor population is occupied by the specific analyte. Sigmoidal-shaped curves were observed over three logarithm units (Fig. S40‡). The data was fit to a linearised form of the Henderson–Hasselbalch, eqn (3). The pβ_{Na+} for **1** are 1.6 and 0.86 in 1 : 1 (v/v) MeOH/H_2O and water, and the pβ_{K+} for **2** are 2.6 and 1.6 in 1 : 1 (v/v) MeOH/H_2O and water, respectively. The pβ_{H+} are 7.4 ± 0.1 and 8.1 ± 0.1 in 1 : 1 (v/v) MeOH/H_2O and water, respectively. The data are tabulated in Table 1.

Table 3 summarises the fluorescence quantum yields (Φ_f), Na^+ and K^+ binding (pβ_{Na+}, pβ_{K+}) and H^+ binding (pβ_{H+}) constants of logic gates **1** and **10–13** (Fig. 3). The data for **10–13** are from published literature in methanol or aqueous alcoholic solution.[4,21,29,31,38] Molecules **10** and **11** are naphthalimide-based H^+-driven and Na^+-driven YES gates, and **12** and **13** are Na^+, H^+-driven two-input AND, and Na^+, H^+, Zn^{2+}-driven three-input AND gates, respectively. Logic gate **1** is reminiscent of de Silva's AND logic gate **12** with its '*receptor$_1$-spacer$_1$-fluorophore-spacer$_2$-receptor$_2$*' connectivity. However, while **12** has a pure ππ* excited state, **1** has a ππ* ICT excited state due to the induced dipole moment with the unsymmetrical fluorophore.

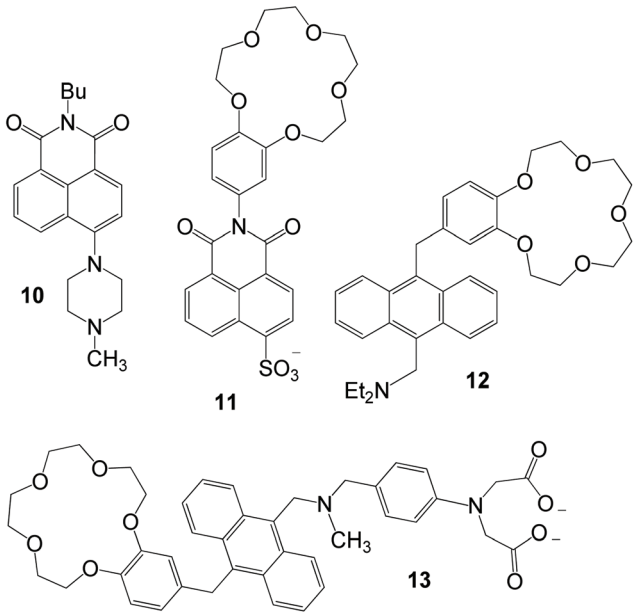

Fig. 3 Naphthalimide and anthracene-based logic gates **10–13**.

Another design difference within **1** and **2** is the virtual C_0-type and C_2-diethylene spacers rather than the C_1-methylene spacers in **12** and **13**.

A reference point for our discussion is the dibutylated aminonaphthalimide dye. It exemplifies a PASS 1 logic gate – between pH 4–12 the Φ_f is constant at 0.23 in 1 : 4 (v/v) methanol/water.[30] Dialkylamino substituents at the 4-amino position contribute towards an enhanced fluorescence on protonation with fluorescence quantum yields of ~0.70 to 0.80, and in the case of **10**, the Φ_f is comparable at 0.58.[31] This value placed an upper limit on the expected Φ_f of **1–3**. The excited state pβ_{H+} of 7.4 is in agreement with **1** corroborating the modular design. Comparison to **11** provides insight into the contribution from the benzo-15-crown-5. The sulfonate enhances water-solubility, and contributes an inductive Hammett effect (σ_p (SO_3^-) = 0.35)[32] towards a favourable PET from the benzo-15-crown-5 to the fluorophore. The pβ_{Na^+} of 1.1 attests to the weaker binding in aqueous media. Two anthracene analogues of **11** with benzo-15-crown-5 have a pβ_{Na^+} of 3.0 and 2.7 in MeOH.[33]

We take the opportunity to compare **1** *versus* **13** in 1 : 1 (v/v) methanol/water and **11**[21] *versus* **13** in water in order to delineate the contribution from the naphthalimide carbonyl towards complexation of Na^+ with the crown ether. In 1 : 1 (v/v)

Table 3 Fluorescence quantum yields ($\Phi_{F_{max}}$) and binding constants (pβ_{M+}) of logic gates **10–13** and **1** in methanol, 50% methanol or water

Parameters	**1**	**1**	**10**[a]	**11**[b]	**12**[c]	**13**[d]	**13**[d]
Solvent	MeOH/H_2O	H_2O	1 : 4 (v/v) MeOH/H_2O	H_2O	MeOH	MeOH/H_2O	H_2O
$\Phi_{F_{max}}$	0.21	0.14	0.58	—	0.22	0.070	0.020
pβ_{Na^+}[e]	1.6	0.86	—	1.1	2.7	0.9	−0.3
pβ_{H^+}[e]	7.5	8.2	7.4	—	8.9	7.8	7.8

$\Phi_{F_{max}}$ in the presence of excess H^+ and/or Na^+ cations. [a] Ref. 31. [b] Ref. 21. [c] Ref. 4. [d] Ref. 38. [e] pβ_{M^+} = $-\log \beta_{M^+}$ where M^+ = Na^+ or H^+.

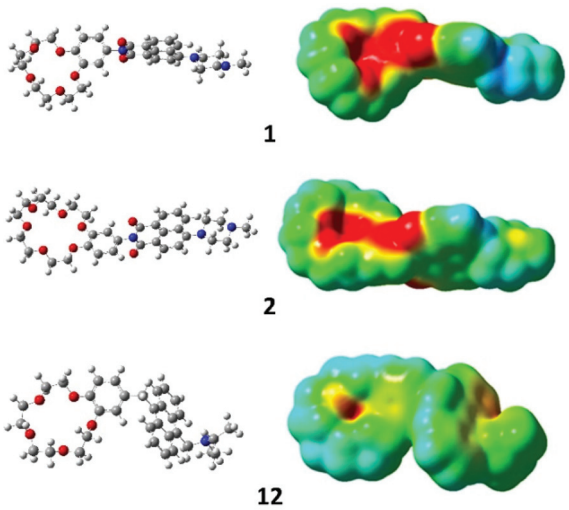

Fig. 4 Geometries and distributions of electrostatic potential (mapped on total electron density) calculated at B3LYP/6-31+g(d,p) theory level in methanol modelled with the IEFPCM approach. Red patches indicate areas bearing negative charge, green are electrically neutral, and blue are positively charged. The identical full colour scale of ±0.05 elemental charge units are used for the sake of comparison.

methanol/water, the $p\beta_{Na^+}$ of **1** and **13** are 1.6 and 0.9, whilst in water the $p\beta_{Na^+}$ of **11** and **13** are 1.1 and −0.3, respectively. Hence, coordination of Na^+ to the naphthalimide carbonyl contributes 0.7–1.4 log units towards the Na^+ binding constant. The origin of this phenomenon was elucidated on the basis of DFT calculations (Fig. 4).

The perpendicular orientation of the organic chromophores (naphthalimide and anthracene moieties) excludes any significant cation π interactions. Both carbonyls of the naphthalimide are highly negative, but one is closer to the benzocrown ether cavity, consequently, there is a slight asymmetry – so a negative charge 'pocket' is formed. Therefore, at least one of the carbonyl groups of the aminonaphthalimide moiety contribute towards the formation of a negatively charged cation-binding pocket in **1** and **2**, whereas the anthracene-based sensor **12** does not show any chromophore-induced charge redistribution. Hence, the aminonaphthalimide is not acting in the traditional manner with respect to the signal analyte binding. In fact, there is a cooperative, synergistic contribution, increasing the negative charge at the receptor site, which enhances cation binding. This is a significant finding as benzocrown ethers are inherently poor at coordinating alkaline metal ions such Na^+ and K^+ in water. Ion-dipole interactions primarily occur at the two oxygen atoms of the 1,2-dimethoxybenzene, and not as much with the aliphatic oxygen atoms.[34] Hence, the presence of a fluorophore carbonyl within the vicinity of the benzocrown increases cation affinity analogous to an object held between four fingers and a thumb (Fig. 4, Compound **1**). Similar phenomena was observed by Valeur with coumarin C153 linked to dibenzo-16-crown-5 and tribenzo-19-crown-6, but in acetonitrile and ethanol, respectively.[35]

Generally, the binding constants and fluorescence emission quantum yields tend to be lower in water than in organic solvents because of differences in solvation energies. Specifically, the effect of solvent polarity on the Φ_f of aminonaphthalimide dyes is attributed to a non-radiative deactivation.[36] Often times, the electron transfer pathway is never fully prevented, which undermines the quality of the Φ_f switching between the *off* and *on* states.[37] For instance, the lower Φ_f of **13** is due to a residual PET from the benzo-15-crown-5 to the excited anthracene as the Na^+ ion does not adequately lower the HOMO level of the benzo-15-crown-5 receptor. 'Lab-on-a-molecule' **13** required 0.50 M Na^+ ($p\beta_{Na^+} = -0.30$) in water to turn on compared to only 0.86 mM ($p\beta_{Na^+} = 3.07$) and 1.12 mM ($p\beta_{Na^+} = 2.95$) for **1** and **11** (Table 3).

The benzocrown derivatives **1** and **2** showed no significant selectivity in water (Fig. S41,‡ Table 2 and Table S1‡). The Φ_f is high at 10^{-4} M H^+ regardless of the presence of the second guest species, whilst at 10^{-9} M H^+ the Φ_f is low and the green fluorescence turned off. This observation is due to the weak electron-donating capability of the benzocrown, as predicted by the Weller equation, and the weaker interaction between the benzocrown receptor and the guest cation. As eluded to earlier, benzocrowns bind cations in water rather weakly (the dibenzo-18-crown-6 equilibrium binding constant for K^+ equals *ca.* 42 in water, 560 in 50% methanol and over 70 000 in methanol).[39]

Therefore, the systems can be considered, in terms of Boolean logic, as H^+-driven YES gates in water where the second input (metal ion) is neglected (Fig. 5). In contrast, the molecules function as Na^+, H^+ and K^+, H^+-driven two-input AND logic gates in 1 : 1 (v/v) MeOH/H_2O. Hence, we have an example of logic function modulation by a change in solvent polarity.[40] The effect is postulated to be a polarity-modulated interaction between the guest and host moieties.

Lastly, we examine the case in water where both chemical inputs *are* considered. According to Table 2 for **1** (and Table S1‡ for **2**), we have a situation where a bright fluorescence is observed for two of the four input conditions. Fluorescence (output 1) is observed when both H^+ and M^+ are high (inputs 1, 1) and when H^+ is high and M^+ is low (inputs 1, 0). These results are characteristic of the output of individual AND and INHIBIT logic gates, respectively. Therefore, **1**

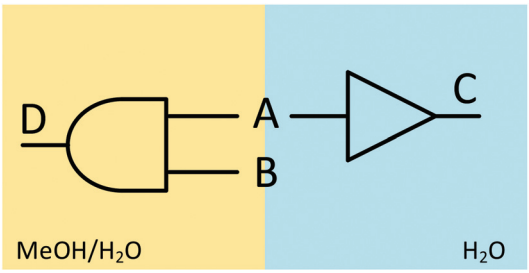

Fig. 5 Combinatorial logic circuit of **1** and **2** with input A = H^+ and input B = Na^+ modulated by solvent polarity in 1 : 1 (v/v) MeOH/H_2O (output D) and H_2O (output C).

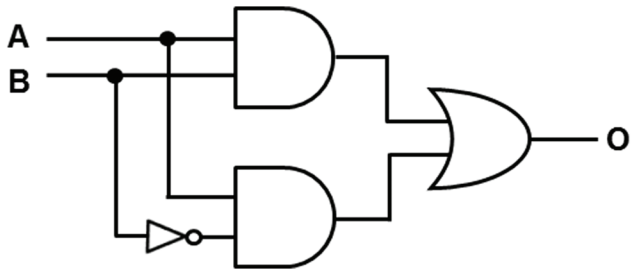

Fig. 6 A combinatorial logic circuit representation of **1** and **2** in water with integrated two-input AND, INHIBIT and OR functions. The output equals the sum-of-products expression O = A·B + A·$\bar{B}$. Accordingly, in Table 2: A = H^+, B = Na^+ and O = Φ_f.

and **2** provide a fluorescent signal according to the Boolean sum-of-products expression A·B + A·$\bar{B}$. In other words, in water, **1** and **2** operate as a combinatorial logic circuit (Fig. 6.) incorporating an AND gate (symbolized by A·B) and an INHIBIT gate (symbolized by A·$\bar{B}$) in parallel and connected sequentially to an OR logic gate (symbolized by +).[41]

Conclusions

Aminonaphthalimide-based molecular logic gates were synthesised with a '*receptor*$_1$-*spacer*$_1$-*fluorophore*-*spacer*$_2$-*receptor*$_2$' format. The molecules incorporate virtual C_0-type and diethylene (C2) spacers, and benzocrown and methylpiperazine receptors. We have shown that: (1) PET from the dimethoxyphenyl electron donor is disrupted on increasing solvent polarity, (2) enhanced crown ether binding occurs *via* Na^+ or K^+ interaction with an aminonaphthalimide carbonyl, and (3) YES and AND Boolean logic gate operations are modulated by Na^+, K^+ and H^+ inputs, in water and methanol/water, respectively. These findings highlight an alternative approach to regulating the logic functions of fluorophores endowed with an ICT excited state and delineate the limitations of the PET/ICT design model. Future studies could dwell into the PET kinetics to better understand the activation barriers and electronic coupling factors.[28] These prototypes hold promise as fluorescent sensors for probing the microenvironment of protein and membrane interfaces,[7,8,42] and as building blocks for the development of more complex logic gates including 'lab-on-a-molecule' systems.[38,43]

Experimental

A list of chemicals and instrumentation are provided in the ESI.‡ The syntheses of **1–3** are shown in Scheme 1. Synthetic procedures and spectroscopic analytical data are given below.

2-(2,3,5,6,8,9,11,12-Octahydrobenzo[*b*][1,4,7,10,13] pentaoxacyclo pentadecin-15-yl)-6-(piperazin-1-yl)-1*H*-benzo[de]isoquinoline-1,3 (2*H*)-dione 15-crown-5 (1)

Benzo-15-crown-5-4-bromo-1,8-naphthalimide (150 mg, 0.28 mmol) and excess methylpiperazine (0.050 mL, 0.45 mmol) were dissolved in 3 mL of DMF. The flask was warmed and stirred at 120 °C for 24 hours. On cooling two drops of tetrabutylammonium hydroxide were added. The solution was diluted with 30 mL of CH_2Cl_2, washed with water (3 × 10 mL) and the solvent removed by rotary evaporation to give a yellow solid, which was purified by column chromatography (102 mg, 65%). R_f (9 : 1 CH_2Cl_2/MeOH) = 0.45; m.p. 232 °C (dec.); ^{1}H NMR (500 MHz, $CDCl_3$, ppm): δ_H 8.61 (d, J = 6.3 Hz, 1H, Ar–H), 8.54 (d, J = 7.5 Hz, 1H, Ar–H), 8.45 (d, J = 7.4 Hz, 1H, Ar–H), 7.71 (m, 1H, Ar–H), 7.26 (s, 1H, Ar–H), 7.00 (d, J = 8.3 Hz, 1H, Ph–H), 6.85 (d, J = 8.2 Hz, 1H, Ph–H), 6.82 (s, 1H, Ph–H), 4.17 (m, 4H, –h($OC\underline{H}_2CH_2O$–)$_2$), 3.91 (m, 4H, –Ph($OCH_2C\underline{H}_2O$–)$_2$), 3.77 (m, 8H, (–OCH_2CH_2O–)$_2$), 3.33 (s, 4H, –N($C\underline{H}_2CH_2$)$_2$$NCH_3$), 2.76 (s, 4H, –N($CH_2C\underline{H}_2$)$_2$$NCH_3$), 2.45 (s, 3H, –$NCH_3$); ^{13}C NMR (126 MHz, $CDCl_3$, ppm): δ_C 46.11, 52.96 (2C), 55.12 (2C), 68.85, 69.04, 69.25, 69.34, 70.48 (2C), 70.91 (2C), 113.89, 114.32, 115.01, 116.68, 121.40, 123.37, 125.65, 126.24, 128.79, 130.23, 130.60, 131.46, 132.95, 148.88, 149.33, 156.20, 164.24, 164.75; IR ν_{max} (NaCl, cm^{-1}): 3072, 2935, 2875, 2853, 2793, 2743, 1694, 1654, 1587, 1517, 1510, 1452, 1373, 1247, 1141, 1079, 1054, 1009, 979, 928, 786, 754; HRMS (ESI TOF): m/z cal. $C_{31}H_{36}N_3O_7$ [M + H] 562.2553, found 562.2557.

2-(2,3,5,6,8,9,11,12,14,15-Decahydrobenzo[*b*][1,4,7,10,13,16] hexa oxacyclooctadecin-18-yl)-6-(4-methylpiperazin-1-yl)-1H-benzo[de] isoquinoline-1,3(2*H*)-dione 18-crown-6 (2)

Compound **2** was prepared similar to **1**. Yellow solid (40 mg, 49%); R_f (9 : 1 CH_2Cl_2/MeOH) = 0.60; m.p. 320 °C (dec.); ^{1}H NMR (500 MHz, $CDCl_3$, ppm): δ_H 8.64 (d, J = 6.2 Hz, 1H, Ar–H), 8.57 (d, J = 6.5 Hz, 1H, Ar–H), 8.47 (d, J = 8.9 Hz, 1H, Ar–H), 7.75 (t, J = 7.3 Hz, 1H, Ar–H), 7.27 (t, J = 9.8 Hz, 1H, Ar–H), 7.04 (d, J = 8.8 Hz, 1H, Ph–H), 6.87 (dd, J = 8.5 Hz, 2.4 Hz, 1H, Ph–H), 6.84 (s, 1H, Ph–H), 4.24 (m, 4H, –Ph($OC\underline{H}_2CH_2O$–)$_2$), 3.98 (m, 4H, –Ph($OCH_2C\underline{H}_2O$)$_2$–), 3.78–3.82 (m, 12H, (–OCH_2CH_2O–)$_3$), 3.37 (s, 4H, –N($C\underline{H}_2CH_2$)$_2$$NCH_3$), 2.79 (s, 4H, –N($CH_2C\underline{H}_2$)$_2$$NCH_3$), 2.48 (s, 3H, –$NCH_3$); ^{13}C NMR (126 MHz, $CDCl_3$, ppm): δ_C 45.97, 53.67 (2C), 55.14 (2C), 68.80, 68.96, 69.38, 69.47, 70.58, 70.61, 70.74 (2C), 70.77, 70.81, 113.71, 114.14, 115.07, 116.72, 121.23, 123.41, 125.68, 126.27, 128.65, 130.26, 130.61, 131.47, 132.94, 148.84, 149.30, 156.19, 164.15, 164.80; IR ν_{max} (KBr, cm^{-1}): 3087, 3035, 2990, 2879, 2766, 2710, 1695, 1660, 1585, 1520, 1516, 1380, 1245, 1127, 1091, 1002, 975, 790, 763; MS (ES-TOF, 2.81 mV) m/z (%): 312 (13), 335(13), 524(32), 525(13), 606(20), 62(30), 628(100); MS (ES-TOF, 298 mV) m/z (%): 312(9), 314(9), 335(12), 337(12), 524 (28), 525(11), 606(20); HRMS (ESI TOF): m/z cal. $C_{33}H_{40}N_3O_8$ [M + H] 606.2815, found 606.2830.

2-(3,4-Dimethoxyphenyl)-6-(4-methylpiperazin-1-yl)-1*H*-benzo [de] isoquinoline-1,3(2*H*)-dione (3)

3,4-Dimethoxyaniline-4-chloro-1,8-naphthalimide (100 mg, 0.27 mmol) and excess methylpiperazine (0.050 mL, 0.45 mmol) were dissolved in 20 mL of DMF and heated at 130 °C for 48 hours. Heptane was added to the DMF solution to form an azeotropic mixture, which was removed by rotary evaporation. The residue was dissolved in CH_2Cl_2, washed

with water (3 × 10 mL) and the CH_2Cl_2 removed by rotary evaporator to yield a yellow solid, which was washed with 10 mL of water and dried under vacuum (82 mg, 70%); R_f (95 : 5 CH_2Cl_2/MeOH) = 0.94; m.p. 230 °C (dec.); ^{1}H NMR (500 MHz, $CDCl_3$, ppm): δ_H 8.63 (d, J = 7.2 Hz, 1H, Ar–H), 8.56 (d, J = 8.0 Hz, 1H, Ar–H), 8.46 (d, J = 8.4 Hz, 1H, Ar–H), 7.73 (t, J = 7.3 Hz, 1H, Ar–H), 7.25 (d, J = 8.0 Hz, 1H, Ar–H), 7.02 (d, J = 8.5 Hz, 1H, Ph–H), 6.88 (d, J = 8.4 Hz, 1H, Ph–H), 6.81 (s, 1H, Ph–H), 3.95 (s, 3H, –OCH_3), 3.88 (s, 3H, –OCH_3), 3.35 (s, 4H, –N($C\underline{H}_2CH_2$)$_2$NCH_3), 2.78 (s, 4H, –N($CH_2C\underline{H}_2$)$_2$NCH_3), 2.47 (s, 3H, –NCH_3); ^{13}C NMR (126 MHz, $CDCl_3$, ppm): δ_C 46.16, 53.02, 55.16, 55.91, 56.04, 111.40, 111.84, 115.05, 116.72, 120.79, 123.42, 125.70, 126.29, 128.37, 130.30, 130.67, 131.52, 133.01, 149.08, 149.57, 156.28, 164.38, 164.90; IR ν_{max} (KBr, cm^{-1}): 3075, 2955, 2853, 2802, 1701, 1649, 1593, 1516, 1381, 1240, 1189, 1002, 783; MS (ES-TOF, 298 mV) m/z (%): 174(3), 432(57), 433(15), 473(32, M + MeCN), 473(65, M + MeCN + Na); HRMS (ESI TOF): m/z cal. $C_{25}H_{26}N_3O_4$ [M + H] 432.1923, found 432.1927.

6-Chloro-2-(2,3,5,6,8,9,11,12-octahydrobenzo[*b*][1,4,7,10,13] penta oxacyclopentadecin-15-yl)-1*H*-benzo[de]isoquinoline-1,3(2*H*)-dione (4)

Compound **4** was prepared similar to **5**. Light brown solid (360 mg, 62%); R_f (9 : 1 CH_2Cl_2/MeOH) = 0.40; m.p. 210–213 °C; ^{1}H NMR (500 MHz, $CDCl_3$, ppm): δ_H: 8.70 (d, J = 7.2 Hz, 1H, Ar–H), 8.66 (d, J = 8.5 Hz, 1H, Ar–H), 8.55 (d, J = 7.9 Hz, 1H, Ar–H), 7.89 (t, J = 8.0 Hz, 1H, Ar–H), 7.86 (d, J = 7.9 Hz, 1H, Ar–H), 7.01 (d, J = 8.5 Hz, 1H, Ph–H), 6.86 (dd, J = 8.5 Hz, 2.4 Hz, 1H, Ph–H), 6.81 (d, J = 2.4 Hz, 1H, Ph–H), 4.18 (m, 4H, –Ph($OC\underline{H}_2CH_2O$–)$_2$), 3.92 (m, 4H, –Ph($OCH_2C\underline{H}_2O$–)$_2$), 3.77 (m, 8H, (–OCH_2CH_2O–)$_2$); ^{13}C NMR (126 MHz, $CDCl_3$, ppm): δ_C 68.98, 69.11, 69.42, 69.51, 70.53, 70.58, 71.04, 71.08, 113.91, 114.23, 121.23, 121.70, 123.21, 127.47, 127.94, 128.12, 129.35, 129.42, 130.93, 131.47, 132.38, 139.37, 149.29, 149.59, 163.74, 164.01; IR ν_{max} (KBr, cm^{-1}): 3080, 3068, 2930, 2874, 2816, 1701, 1663, 1589, 1574, 1516, 1506, 1371, 1242, 1128, 1055, 785, 765, 750; MS (ES-TOF, 2.82 mV) m/z (%): 177(100), 178(13), 224(9), 334 (20), 498(M + H, 11), 515(35), 520 (M + Na, 85), 521(25), 522 (32), 523(9); HRMS m/z cal. $C_{26}H_{24}NO_7NaCl$ [M + Na] 520.1139, found 520.1146.

6-Bromo-2-(2,3,5,6,8,9,11,12-octahydrobenzo[*b*][1,4,7,10,13] penta oxacyclopentadecin-15-yl)-1*H*-benzo[de]isoquinoline-1,3(2*H*)-dione (5)

4-Aminobenzo-15-crown-5 (130 mg, 0.45 mmol) and 4-bromo-1,8-naphthalic anhydride (270 mg, 0.97 mmol) were dissolved in 5 mL of 2-methoxyethanol in a 100 mL round-bottom flask. The reaction mixture was stirred and heated at 110 °C for 20 hours. The solvent was removed by rotary evaporation. Washing with cold 2-methoxyethanol gave an off-white powder (180 mg, 73%). R_f (9 : 1 CH_2Cl_2/MeOH) = 0.41; m.p. 235–238 °C; ^{1}H NMR (500 MHz, $CDCl_3$, ppm): δ_H 8.70 (d, J = 7.2 Hz, 1H, Ar–H), 8.63 (d, J = 8.4 Hz, 1H, Ar–H), 8.45 (d, J = 7.8 Hz, 1H, Ar–H), 8.08 (d, J = 7.9 Hz, 1H, Ar–H), 7.88 (t, J = 7.9 Hz, 1H, Ar–H), 7.01 (d, J = 8.5 Hz, 1H, Ph–H), 6.86 (dd, J = 8.5 Hz, 2.2 Hz, 1H, Ph–H), 6.81 (d, J = 2.2 Hz, 1H, Ph–H), 4.18 (m, 4H, –Ph($OC\underline{H}_2CH_2O$–)$_2$), 3.92 (m, 4H, –Ph($OCH_2C\underline{H}_2O$–)$_2$), 3.78 (d, J = 7.3 Hz, 8H, (–OCH_2CH_2O–)$_2$); ^{13}C NMR (126 MHz, $CDCl_3$, ppm): δ_C 69.16, 69.31, 69.56, 69.66, 70.63, 70.67, 71.27, 71.30, 114.08, 114.32, 121.20, 122.40, 123.27, 128.10, 128.18, 129.30, 130.61, 130.76, 131.21, 131.57, 132.42, 133.57, 149.43, 149.74, 163.86, 163.90; IR ν_{max} (KBr, cm^{-1}): 3080, 3067, 2930, 2872, 2816, 1701, 1662, 1587, 1518, 1506, 1367, 1240, 1144, 1047, 785, 766, 750; MS (ES-TOF, 2.81 mV) m/z (%): 177(100), 178(13), 224(9), 391(4), 542(M, 10), 544(11), 559(28), 561(29), 564(73), 565(21), 566(72), 567(21); HRMS m/z cal. $C_{26}H_{24}NO_7NaBr$ [M + Na] 564.0634, found 564.0657.

6-Chloro-2-(2,3,5,6,8,9,11,12,14,15-decahydrobenzo[*b*] [1,4,7,10, 13,16]hexaoxacyclooctadecin-18-yl)-1*H*-benzo[de]isoquinoline-1,3(2*H*)-dione (6)

Compound **6** was prepared similar to **5**. White solid (140 mg, 61%); R_f (9 : 1 CH_2Cl_2/MeOH) = 0.28; m.p. 202–206 °C; ^{1}H NMR (500 MHz, $CDCl_3$, ppm): δ_H 8.70 (d, J = 7.2 Hz, 1H, Ar–H), 8.67 (d, J = 8.5 Hz, 1H, Ar–H), 8.55 (d, J = 7.9 Hz, 1H, Ar–H), 7.89 (m, J = 7.7 Hz, 1H, Ar–H), 7.87 (d, J = 8.0 Hz, 1H, Ar–H), 7.02 (d, J = 8.5 Hz, 1H, Ph–H), 6.86 (dd, J = 2.3 Hz, 8.5 Hz, 1H, Ph–H), 6.81 (d, J = 2.3 Hz, 1H, Ph–H), 4.20 (m, 4H, –Ph($OC\underline{H}_2CH_2O$–)$_2$), 3.95 (m, 4H, –Ph($OCH_2C\underline{H}_2O$)$_2$–), 3.73–3.79 (m, 12H, (–OCH_2CH_2O–)$_3$); ^{13}C NMR (126 MHz, $CDCl_3$, ppm): δ_C 69.03, 69.13, 69.43, 69.52, 70.65, 70.69, 70.81 (2C), 70.86, 70.93, 113.76, 114.05, 121.11, 121.75, 123.26, 127.48, 127.94, 128.03, 129.39, 129.45, 130.94, 131.50, 132.41, 139.36, 149.13, 149.43, 163.77, 164.03; IR ν_{max} (KBr, cm^{-1}): 3084, 3071, 2934, 2883, 2876, 1705, 1683, 1663, 1589, 1516, 1506, 1373, 1242, 1126, 1083, 959, 786; MS (ES-TOF, 0.395 mV) m/z (%): 177(5), 559(22), 560(21), 561(20), 564(M + Na, 100), 566(36), 567(11); HRMS m/z cal. $C_{28}H_{28}NO_8NaCl$ 564.1401, found 564.1405.

6-Bromo-2-(2,3,5,6,8,9,11,12,14,15-decahydrobenzo[*b*] [1,4,7,10, 13,16]hexaoxacyclooctadecin-18-yl)-1*H*-benzo[de] isoquinoline-1,3(2*H*)-dione (7)

Compound **7** was prepared similar to **5**. Off-white solid (100 mg, 57%); R_f (9 : 1 CH_2Cl_2/MeOH) = 0.35; m.p. 197 °C (dec.); ^{1}H NMR (500 MHz, $CDCl_3$, ppm): δ_H 8.71 (d, J = 7.1 Hz, 1H, Ar–H), 8.62 (d, J = 8.5 Hz, 1H, Ar–H), 8.46 (d, J = 7.8 Hz, 1H, Ar–H), 8.06 (d, J = 7.9 Hz, 1H, Ar–H), 7.88 (t, J = 8.0 Hz, 1H, Ar–H), 7.02 (d, J = 8.4 Hz, 1H, Ph–H), 6.87 (dd, J = 8.3 Hz, 2.3 Hz, 1H, Ph–H), 6.82 (d, J = 2.4 Hz, 1H, Ph–H), 4.23 (m, 4H, –Ph($OC\underline{H}_2CH_2O$–)$_2$), 3.92 (m, 4H, –Ph($OCH_2C\underline{H}_2O$)$_2$–), 3.70–3.79 (m, 12H, (–OCH_2CH_2O–)$_3$); ^{13}C NMR (126 MHz, $CDCl_3$, ppm): δ_C 68.18, 69.29, 69.51, 69.60, 70.74, 70.78, 70.89 (2C), 70.96, 70.99, 114.00, 114.23, 121.14, 122.42, 123.30, 128.06, 128.19, 129.34, 130.62, 130.80, 131.22, 131.70, 132.43, 133.59, 149.25, 149.56, 163.88, 163.91; IR ν_{max} (KBr, cm^{-1}): 3080, 3079, 2930, 2875, 1699, 1680, 1662, 1595, 1520, 1516, 1370, 1242, 1130, 1087, 950, 785; MS (ES-TOF, 2.81 mV) m/z (%): 162(7), 224(18), 338(13), 390(86), 391(28), 418(13), 482(37), 511(24), 529(37), 603(97), 605(100), 610(63), 611(25); HRMS m/z cal. $C_{28}H_{28}NO_8NaBr$ [M + Na] 608.0896, found 608.0904.

6-Chloro-2-(3,4-dimethoxyphenyl)-1*H*-benzo[de]isoquinoline-1,3 (2*H*)-dione (8)

4-Chloro-1,8-naphthalimide anhydride (1.7 g, 7.3 mmol) and 3,4-dimethoxyaniline (2.6 g, 11 mmol) were dissolved in 3 mL of glacial acetic acid and heated at 130 °C for 48 hours. After cooling, hexane was added and the azeotropic mixture removed by rotary evaporation. The product was washed with acetone and dried by suction filtration to yield a white solid (2.3 g, 85%), R_f = 0.85 (9 : 1 CH_2Cl_2/CH_3OH), m.p. = 287.5–289.0 °C (dec.); ^{1}H NMR (500 MHz, $CDCl_3$, ppm): δ_H 8.71 (dd, 1H, J = 7.3 Hz, 1.1 Hz, Ar–H), 8.66 (dd, 1H, J = 8.5 Hz, 1.1 Hz, Ar–H), 8.55 (d, 1H, J = 7.8 Hz, Ar–H), 7.89 (dd, 1H, J = 8.5 Hz, 7.4 Hz, Ar–H), 7.86 (d, 1H, J = 7.8 Hz, Ar–H), 7.03 (d, 1H, J = 8.4 Hz, Ph–H), 6.88 (dd, 1H, J = 8.6 Hz, 2.4 Hz, Ph–H), 6.81 (d, 1H, J = 2.6 Hz, Ph–H), 3.95 (s, 3H, –OCH_3), 3.88 (s, 3H, –OCH_3); ^{13}C NMR (126 MHz, $CDCl_3$, ppm): δ_C 55.92, 56.05, 111.37, 111.65, 120.65, 121.68, 123.20, 127.72, 127.90, 129.34, 129.40, 130.92, 131.46, 132.37, 139.36, 149.25, 149.61, 163.79, 164.05; IR ν_{max} (KBr, cm^{-1}): 3076, 2937, 2836, 1713, 1658, 1591, 1514, 1370, 1241, 1138, 1024, 781, 747; MS (ES-TOF) m/z (%): 205(15), 243(10), 299(15), 368(100), 369(22), 370(34); HRMS m/z cal. $C_{20}H_{15}NO_4Cl$ 368.0690, found 368.0691.

6-Bromo-2-(3,4-dimethoxyphenyl)-1*H*-benzo[de]isoquinoline-1,3 (2*H*)-dione (9)

Compound **9** was prepared similar to **8**. Off-white solid (534 mg, 72%); R_f = 0.90 (9 : 1 CH_2Cl_2/CH_3OH), m.p. = 280 °C (dec.); ^{1}H NMR (500 MHz, $CDCl_3$, ppm): δ_H 8.71 (dd, 1H, J = 7.0 Hz, 0.9 Hz, Ar–H), 8.64 (dd, 1H, J = 8.6 Hz, 0.7 Hz, Ar–H), 8.46 (d, 1H, J = 7.8 Hz, Ar–H), 8.08 (d, 1H, J = 7.9 Hz, Ar–H), 7.89 (dd, 1H, J = 8.3 Hz, 7.5 Hz, Ar–H), 7.03 (d, 1H, J = 8.5 Hz, Ph–H), 6.89 (dd, 1H, J = 8.4 Hz, 2.3 Hz, Ph–H), 6.81 (d, 1H, J = 2.3 Hz, Ph–H), 3.95 (s, 3H, –OCH_3), 3.88 (s, 3H, –OCH_3); ^{13}C NMR: (126 MHz, $CDCl_3$, ppm): δ_C 55.97, 56.07, 111.43, 111.67, 120.69, 122.04, 123.28, 127.75, 128.20, 129.35, 130.69, 130.81, 131.24, 131.62, 132.48, 133.65, 149.31, 163.84, 163.99, 164.03; IR ν_{max} (KBr, cm^{-1}): 3075, 2963, 2835, 1706, 1659, 1513, 1368, 1239, 1139, 1028, 780; MS (ES-TOF) m/z (%): 414(100), 412(97), 240(10), HRMS cal. $C_{20}H_{15}NO_4Br$ 412.0184, found 412.0176.

DFT calculations were performed using Gaussian 09 Revision E.01 software package using standard B3LYP functional and 6-31+g(d,p) basis.[44] The Polarizable Continuum Model using the integral equation formalism variant (IEFPCM) was used to account for solvent effects, with methanol as a solvent.[45] Chemical names were obtained using Chemdraw Ultra version 12.0.2.1076.

Conflicts of interest

There are no conflicts of interest to declare.

Acknowledgements

Financial support is gratefully acknowledged from the University of Malta and the Strategic Educational Pathways Scholarship (Malta) program part-financed by the European Social Fund (ESF) under Operational Programme II – Cohesion Policy 2007-2013. KS acknowledges financing from the National Science Centre (Poland) under contract UMO-2015/17/B/ST8/01783. DFT calculations were performed at the PL-Grid Infrastructure (Academic Computing Centre CYFRONET AGH) under computational grant GRAPHENE5. Prof. Robert M. Borg is appreciatively thanked for NMR training and assistance.

References

1 (*a*) A. P. de Silva, *Molecular Logic-based Computation*, The Royal Society of Chemistry, Cambridge, UK, 2013; (*b*) K. Szaciłowski, *Infochemistry*, Wiley-VCH, Chichester, UK, 2012; (*c*) *Molecular and Supramolecular Information Processing: From Molecular Switches to Logic Systems*, ed. E. Katz, Wiley-VCH Verlag, Weinheim, Germany, 2012; (*d*) *Biomolecular Information Processing: From Logic Systems to Smart Sensors and Actuators*, ed. E. Katz, Wiley-VCH, Weinheim, Germany, 2012.

2 A. P. de Silva, H. Q. N. Gunaratne and C. P. McCoy, *Nature*, 1993, **364**, 42.

3 (*a*) A. P. de Silva, T. S. Moody and G. D. Wright, *Analyst*, 2009, **134**, 2385; (*b*) A. P. de Silva, *J. Phys. Chem. Lett.*, 2011, **2**, 2865.

4 A. P. de Silva, H. Q. N. Gunaratne and C. P. McCoy, *J. Am. Chem. Soc.*, 1997, **119**, 7891.

5 (*a*) S. Erbas-Cakmak, T. Gunnlaugsson, S. Kolemen, T. D. James, A. C. Sedgwick, J. Yoon and E. U. Akkaya, *Chem. Soc. Rev.*, 2018, **47**, 2266; (*b*) J. Andréasson and U. Pischel, *Chem. Soc. Rev.*, 2018, **47**, 2228; (*c*) B. Daly, J. Ling and A. P. de Silva, *Chem. Soc. Rev.*, 2015, **44**, 4203; (*d*) J. Ling, B. Daly, V. A. D. Silverson and A. P. de Silva, *Chem. Commun.*, 2015, **51**, 8403.

6 G. W. Gokel, W. M. Leevy and M. E. Weber, *Chem. Rev.*, 2004, **104**, 2723.

7 (*a*) S. Uchiyama, K. Yano, E. Fukatsu and A. P. de Silva, *Chem. – Eur. J.*, 2019, **25**, 8522; (*b*) S. Uchiyama, G. D. McClean, K. Iwai and A. P. de Silva, *J. Am. Chem. Soc.*, 2005, **127**, 8920.

8 B. McLaughlin, E. M. Surender, G. D. Wright, B. Daly and A. P. de Silva, *Chem. Commun.*, 2018, **54**, 1319.

9 S. Ozlem and E. U. Akkaya, *J. Am. Chem. Soc.*, 2009, **131**, 48.

10 E. V. Anslyn and D. D. Dougherty, *Modern Physical Organic Chemistry*, University Science Books, Sausalito, California, 2006.

11 (*a*) X. Sun, B. M. Chapin, P. Metola, B. Collins, B. Wang, T. D. James and E. V. Anslyn, *Nat. Chem.*, 2019, **11**, 768; (*b*) X. Sun, T. D. James and E. V. Anslyn, *J. Am. Chem. Soc.*, 2018, **140**, 2348; (*c*) B. M. Chapin, P. Metola, S. L. Vankayala, H. L. Woodcock, T. J. Mooibroek, V. M. Lynch, J. D. Larkin and E. V. Anslyn, *J. Am. Chem. Soc.*, 2017, **139**, 5568.

12 (*a*) T. D. James, K. R. A. S. Sandanayake and S. Shinkai, *J. Chem. Soc., Chem. Commun.*, 1994, 477; (*b*) T. D. James, K. R. A. S. Sandanayake and S. Shinkai, *Angew. Chem., Int. Ed. Engl.*, 1994, **33**, 2207.

13 (*a*) R. A. Bissell, A. P. de Silva, H. Q. N. Gunaratne, P. L. M. Lynch, G. E. M. Maguire and K. R. A. S. Sandanayake, *Chem. Soc. Rev.*, 1992, **21**, 187; (*b*) X. Jia, Y. Yang, Y. Xu and X. Qian, *Pure Appl. Chem.*, 2014, **86**, 1237; (*c*) W. Chi, J. Chen, Q. Qiao, Y. Gao, Z. Xub and X. Liu, *Phys. Chem. Chem. Phys.*, 2019, **21**, 16798.

14 (*a*) P. Nandhikonda, M. P. Begaye, Z. Cao and M. D. Heagy, *Org. Biomol. Chem.*, 2010, **8**, 3195; (*b*) R. K. Meka and M. D. Heagy, *J. Org. Chem.*, 2017, **82**, 12153.

15 S. Sasaki, G. P. C. Drummen and G. Konishi, *J. Mater. Chem. C*, 2016, **4**, 2731.

16 P. A. Panchenko, O. A. Fedorova and Y. V. Fedorov, *Russ. Chem. Rev.*, 2014, **83**, 155.

17 (*a*) P. A. Panchenko, Y. V. Fedorov, O. A. Fedorova and G. Jonusauskas, *Dyes Pigm.*, 2013, **98**, 347; (*b*) P. A. Panchenko, Y. V. Fedorov, O. A. Fedorova and G. Jonusauskas, *Phys. Chem. Chem. Phys.*, 2015, **17**, 22749; (*c*) P. A. Panchenko, Y. V. Fedorov, V. P. Perevalov, G. Jonusauskas and O. A. Fedorova, *J. Phys. Chem. A*, 2010, **114**, 4118.

18 P. A. Panchenko, Y. V. Fedorov and O. A. Fedorova, *J. Photochem. Photobiol., A*, 2018, **364**, 124.

19 P. A. Panchenko, A. S. Polyakova, Y. V. Fedorov and O. A. Fedorova, *Mendeleev Commun.*, 2019, **29**, 155.

20 C. Hou, A. M. Urbanec and H. Cao, *Tetrahedron Lett.*, 2011, **52**, 4903.

21 P. Nandhikonda, M. P. Begaye and M. D. Heagy, *Tetrahedron Lett.*, 2009, **50**, 2459.

22 (*a*) H. He, M. A. Mortellaro, M. J. P. Leiner, S. T. Young, R. J. Fraatz and J. K. Tusa, *Anal. Chem.*, 2003, **75**, 549; (*b*) T. Gunnlaugsson, M. Nieuwenhuyzen, L. Richard and V. Thoss, *J. Chem. Soc., Perkin Trans. 2*, 2002, 141; (*c*) T. Gunnlaugsson, M. Nieuwenhuyzen, L. Richard and V. Thoss, *Tetrahedron Lett.*, 2001, **42**, 4725.

23 (*a*) H. He, M. A. Mortellaro, M. J. P. Leiner, S. T. Young, R. J. Fraatz and J. K. Tusa, *Anal. Chem.*, 2003, **75**, 549; (*b*) J. K. Tusa and H. He, *J. Mater. Chem.*, 2005, **2**, 2865; (*c*) D. C. Magri, *Metal Ion Sensing for Biomedical Uses, in Molecular and Supramolecular Information Processing: From Molecular Switches to Logic Systems*, ed. E. Katz, Wiley-VCH, Weinheim, 2012, ch. 3, p. 79.

24 M. F. Harris and J. L. Logan, *J. Chem. Educ.*, 2014, **91**, 915.

25 J. M. A. Spiteri, C. J. Mallia, G. J. Scerri and D. C. Magri, *Org. Biomol. Chem.*, 2017, **15**, 10116.

26 A. Weller, *Pure Appl. Chem.*, 1968, **16**, 115. E_{OX} is the oxidation potentials of 1,2-dimethoxybenzene (1.45 eV) or tertiary amine (1.15 eV), E_{RED} is the reduction potential of naphthalimide (−1.57 eV), E_S is the excited state singlet energy of naphthalimide (2.55 eV) and $e^2/\varepsilon r$ is the coulombic term (0.10 eV) where e is the electric charge of an electron, ε is the dielectric constant and r the separation distance. Potentials are versus SCE in acetonitrile.

27 (*a*) D. C. Magri, J. F. Callan, N. D. McClenaghan, A. P. de Silva, D. B. Fox and K. R. A. S. Sandanayake, *J. Fluoresc.*, 2005, **15**, 769; (*b*) Z. R. Grabowski and J. Dobkowski, *Pure Appl. Chem.*, 1983, **55**, 245.

28 J. C. Spiteri, S. A. Denisov, G. Jonusauskas, S. Klejna, K. Szaciłowski, N. D. McClenaghan and D. C. Magri, *Org. Biomol. Chem.*, 2018, **16**, 6195.

29 D. C. Magri and A. P. de Silva, *New J. Chem.*, 2010, **34**, 476.

30 A. P. de Silva, H. Q. N. Gunaratne, J. L. Habib-Jiwan, C. P. McCoy, T. E. Rice and J. P. Soumillion, *Angew. Chem., Int. Ed. Engl.*, 1995, **107**, 1728.

31 S. Zheng, P. L. M. Lynch, T. E. Rice, T. S. Moody, H. Q. N. Gunaratne and A. P. de Silva, *Photochem. Photobiol. Sci.*, 2012, **11**, 1675.

32 C. Hansch, A. Leo and R. W. Taft, *Chem. Rev.*, 1991, **91**, 165.

33 A. P. de Silva and K. R. A. S. Sandanayake, *J. Chem. Soc., Chem. Commun.*, 1989, 1183.

34 J. W. Steed, *Coord. Chem. Rev.*, 2001, **215**, 171.

35 (*a*) J. Bourson, J. Pouget and B. Valeur, *J. Phys. Chem.*, 1993, **97**, 4552; (*b*) I. Leray, J. L. Habib-Jiwan, C. Branger, J. P. Soumillion and B. Valeur, *J. Photochem. Photobiol., A*, 2000, **135**, 163.

36 (*a*) Z. Li, Q. Yang, R. Chang, G. Ma, M. Chen and W. Zhang, *Dyes Pigm.*, 2011, **88**, 307; (*b*) E. Krystkowiak, K. Dobek and A. Maciejewski, *J. Photochem. Photobiol., A*, 2006, **184**, 250; (*c*) D. Yuan and R. G. Brown, *J. Phys. Chem. A*, 1997, **101**, 3461.

37 H. Kawai, T. Nagamura, T. Mori and K. Yoshida, *J. Phys. Chem. A*, 1999, **103**, 660.

38 D. C. Magri, G. J. Brown, G. D. McClean and A. P. de Silva, *J. Am. Chem. Soc.*, 2006, **128**, 4950.

39 R. Konášová, J. Jaklová Dytrtová and V. Kašička, *J. Sep. Sci.*, 2016, **39**, 4429.

40 (*a*) A. P. de Silva and K. R. A. S. Sandanayake, *Tetrahedron Lett.*, 1991, **32**, 421; (*b*) J. Hatai, S. Pal, G. P. Jose, T. Sengupta and S. Bandyopadhyay, *RSC Adv.*, 2012, **2**, 7033.

41 T. Konry and D. R. Walt, *J. Am. Chem. Soc.*, 2009, **131**, 13232. The truth table reported for two-input AND-INH-OR is incomplete. One row of entries (all zeros) is missing. For an example of a three-input AND-INH-OR logic gate see ref. 43*b*.

42 (*a*) S. Bhunia, S. Kumar and P. Purkayastha, *ACS Omega*, 2019, **4**, 2523; (*b*) K. J. Cao, K. M. Elbel, J. L. Cifelli, J. Cirera, C. J. Sigurdson, F. Paesani, E. A. Theodorakis and J. Yang, *Sci. Rep.*, 2018, **8**, 6950.

43 (*a*) G. J. Scerri, J. C. Spiteri, C. J. Mallia and D. C. Magri, *Chem. Commun.*, 2019, **55**, 4961; (*b*) D. C. Magri and J. C. Spiteri, *Org. Biomol. Chem.*, 2017, **15**, 6706; (*c*) D. C. Magri, M. Camilleri Fava and C. J. Mallia, *Chem. Commun.*, 2014, **50**, 1009.

44 M. J. Frisch, G. W. Trucks, H. B. Schlegel, G. E. Scuseria, M. A. Robb, J. R. Cheeseman, G. Scalmani, V. Barone,

B. Mennucci, G. A. Petersson, H. Nakatsuji, M. Caricato, X. Li, H. P. Hratchian, A. F. Izmaylov, J. Bloino, G. Zheng, J. L. Sonnenberg, M. Hada, M. Ehara, K. Toyota, R. Fukuda, J. Hasegawa, M. Ishida, T. Nakajima, Y. Honda, O. Kitao, H. Nakai, T. Vreven, J. A. Montgomery Jr., J. E. Peralta, F. Ogliaro, M. Bearpark, J. J. Heyd, E. Brothers, K. N. Kudin, V. N. Staroverov, T. Keith, R. Kobayashi, J. Normand, K. Raghavachari, A. Rendell, J. C. Burant, S. S. Iyengar, J. Tomasi, M. Cossi, N. Rega, J. M. Millam, M. Klene, J. E. Knox, J. B. Cross, V. Bakken, C. Adamo, J. Jaramillo, R. Gomperts, R. E. Stratmann, O. Yazyev, A. J. Austin, R. Cammi, C. Pomelli, J. W. Ochterski, R. L. Martin, K. Morokuma, V. G. Zakrzewski, G. A. Voth, P. Salvador, J. J. Dannenberg, S. Dapprich, A. D. Daniels, O. Farkas, J. B. Foresman, J. V. Ortiz, J. Cioslowski and D. J. Fox, *Gaussian 09, Revision E.01*, Gaussian, Inc., Wallingford, CT, 2013.

45 S. Miertuš, E. Scrocco and J. Tomasi, *Chem. Phys.*, 1981, **55**, 117.